



Destruction of acenaphthene, fluorene, anthracene and pyrene by a dc gliding arc plasma reactor

Liang Yu^a, Xin Tu^b, Xiaodong Li^a, Yu Wang^a, Yong Chi^a, Jianhua Yan^{a,*}

^a State Key Laboratory of Clean Energy Utilization, Zhejiang University, Hangzhou, 310027, China

^b School of Chemistry, The University of Manchester, Oxford Road, Manchester, M13 9PL, UK

ARTICLE INFO

Article history:

Received 5 January 2010

Received in revised form 22 March 2010

Accepted 13 April 2010

Available online 18 April 2010

Keywords:

Polycyclic aromatic hydrocarbons

Destruction

Gliding arc

Non-thermal plasma

ABSTRACT

In this study, four kinds of PAHs (polycyclic aromatic hydrocarbons) i.e. acenaphthene, fluorene, anthracene and pyrene are used as targets for investigation of PAHs treatment process assisted by dc gliding arc discharge. The effects of carrier gas and external resistance on the PAHs decomposition process are discussed. The results indicate that the destruction rate can be achieved to the highest with the carrier gas of oxygen and the external resistance of 50 k Ω independent of type of PAHs. Furthermore, experimental results suggest that destruction energy efficiency of gliding arc plasma would be improved by treating higher concentration pollutants. Based on the analysis of experimental results, possible destruction mechanisms in different gas discharge are discussed.

© 2010 Elsevier B.V. All rights reserved.

1. Introduction

Incomplete combustion of fossil fuel or municipal solid waste (MSW) may lead to release many kinds of persistent organic pollutants (POPs) such as polycyclic aromatic hydrocarbons (PAHs), polychlorinated dibenzo-p-dioxines (PCDDs), polychlorinated dibenzofuran (PCDFs) [1]. PAHs and PCDD/Fs have been designated as priority pollutants by US EPA and attracted increasing attention due to their contribution to environmental and health problems [2]. Many countries have legislated strict laws on these kind of POPs emission. Therefore, it is necessary to develop friendly technologies to destruct POPs. In this study, we focus our attention on the PAHs destruction technology.

In recent years, several technologies have been utilized to remove PAHs from the sewage sludge, contaminated soils and wastewater. Bioremediation has received wide acceptance as a viable and low-cost treatment method for remediation soils and water polluted by PAHs for many years. However, biodegradation-based technologies are usually long-term processes which cost several weeks [3]. In addition, bioremediation often has limited applicability when soils or sewage sludge are contaminated with complex mixtures of highly PAHs. In order to overcome these disadvantages, scientists have developed kinds of new technologies to destruct PAHs. Nam et al. developed a new method, which combined biodegradation and Fenton reaction, to enhance the PAHs

degradation process in soils [4]. Photocatalytic degradation of PAHs on soils surface using TiO₂ under UV light was studied by Zhang et al., which concluded that catalyst TiO₂ can accelerate the PAHs photodegradation speed for 3–4 times [5]. Owing to having large number of energetic electrons and reactive radicals such as OH, O and H, electron beam irradiation has been applied to PAHs destruction in sewage sludge and the destruction rate of PAHs was reported to be about 90% at absorbed dose 5 kGy [6]. The aforementioned technologies are mainly used for destruction of PAHs in solid or liquid phase and a few publications are concerning with PAHs removal in gas flow. We have ever studied the degradation of PAHs and soot particles, released from polyethylene (PE) and polyvinyl chloride (PVC) combustion in a laboratory-scale drop tube furnace, using an ac gliding arc reactor [7]. The results of this research indicated that the PAHs removal rate can be achieved up to 74.4%. However, degradation products and destruction mechanisms were not discussed in that work. Recently, we have developed a dc gliding arc system for the decomposition of PAHs. The specific PAHs decomposition processes [8], dc gliding arc reactor performance and destruction mechanisms are investigated in our further research. In this study, four kinds of PAHs destruction mechanisms are discussed based on a qualitative and quantitative analysis of products. Additionally, a comparative assessment of the gliding arc reactor performance on destruction energy efficiency under different working conditions is done.

As an alternative approach, non-equilibrium plasma technologies have been utilized for volatile organic compounds (VOCs) abatement, wastewater treatment and energy conversion for many years and received increasing attentions [9–10]. Because of the

* Corresponding author. Tel.: +86 571 87952443; fax: +86 571 87952438.

E-mail addresses: yanjh@zju.edu.cn, yuliang@zju.edu.cn (J. Yan).

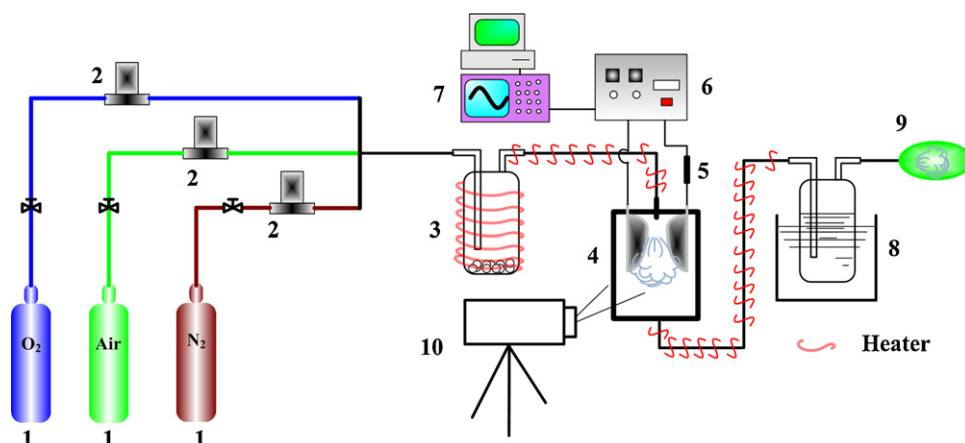


Fig. 1. Experimental setup: 1. gas source, 2. mass flow controller, 3. PAHs source, 4. gliding arc reactor, 5. external resistor, 6. power source, 7. oscilloscope, 8. absorption bottle containing hexane, 9. gas bag; 10. high speed camera.

large number of high energy electrons and radicals and relative low gas temperature, non-equilibrium plasma is regarded as a promising technology for gas phase pollutants destruction. In this study, we study the four kinds of PAHs decomposition processes by one of non-thermal plasmas, namely gliding arc discharge, which has been utilized for abatement of some other gas pollutants and considered as an efficient kind of non-thermal plasma by many scientists.

2. Experimental

2.1. Experimental setup

The experimental setup shown in Fig. 1 mainly consists of PAHs-containing gas generation system, a dc gliding arc plasma reactor and an analysis system. PAHs powders are placed in glass bottle and be heated to set temperature. The temperature of transfer pipe in the experiment is kept at 130 °C. The vaporized PAHs are carried by gas flow at 6 l/min and sprayed into gliding arc plasma system which consists of a dc power supply (0–6150 V, 900 W), an external resistance bank (50–93 kΩ) and a quartz gliding arc reactor. Compared with the PE and PVC combustion system [11], this gas phase PAHs-generations system are more stable. The arc voltage and current are measured by using a current probe (Tektronix, TCP303) and a high voltage probe (Tektronix, P6015A), respectively. The electrical signals are sampled synchronously through a digital oscilloscope (Tektronix, TDS2024). The spatial evolution of the gliding arc column is recorded by an HG-100K high speed camera. Emission spectra of the gliding arc discharge are measured by an optical fiber connected with a SBP300 spectrometer. To collect the reaction products, Post-destroyed gas flows pass through the absorption bottle containing hexane. We carried out each experiment for 3 min. Every experiment is started after 20 min stabilization without discharge.

2.2. Materials and methods

Four kinds of PAHs as test pollutants, namely acenaphthene (AcP), fluorene (Flu), anthracene (AnT) and pyrene (Pyr), are purchased from Sigma–Aldrich (HPLC grade), Japan, and are used without further purification. Hexane (analytical grade) is purchased from Sinopharm Chemical Reagent Co. Ltd., China. In these experiments, nitrogen, air and oxygen are used as carrier gas and external resistance varies from 50 kΩ to 93 kΩ. Post-destroyed products in hexane are analyzed by gas chromatography with mass spec-

trometry detection (GC/MS). The off-gas is analyzed by a FTIR spectrometer.

2.3. Gliding arc gas discharge

Fig. 2 presents the photographs of gliding arc gas discharge recorded by common speed camera and high speed camera (5000 frames/s). The gliding arc gas discharge produces a plasma region characterized by periodic arc movement between at least two electrodes. This type of plasma starts at the shortest gap between electrodes by an initial breakdown of introduced gas when the power source provides high enough voltage between electrodes. Then the arc is pushed downstream by the gas flow and glides along the electrode surface until it quenches. After the decay of discharge, there is a new breakdown at the narrowest gap and the cycle repeats. This periodic discharge evolves during a cycle from arc to transitional discharge with a relative high level of electron density [12]. Electrical signals and an emission spectrum of a nitrogen discharge are shown in Figs. 3 and 4, respectively. An opposite variation tendency can be observed from arc voltage and arc current signals in one period presented in Fig. 3. During the arc evolution, the arc voltage increases and arc current decreases due to increase of discharge length. In Fig. 4, it is obvious that the 300–400 nm scans are predominated by the $N_2(C^3\Pi_u \rightarrow B^3\Pi_u)$ 2nd positive system, which indicates that electronic excited state of nitrogen molecules abound in a nitrogen gliding discharge. Nowadays, gliding arc plasma has attracted considerable interest on its

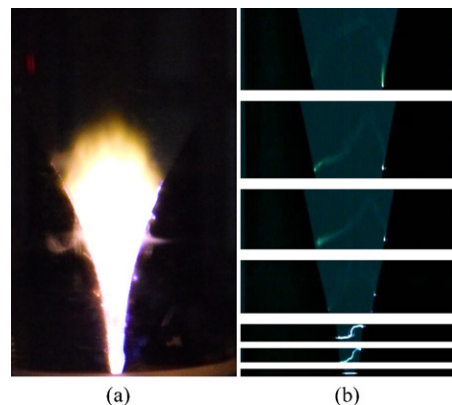


Fig. 2. Photographs of gliding arc discharge recorded by common (a) and high speed (b) cameras.

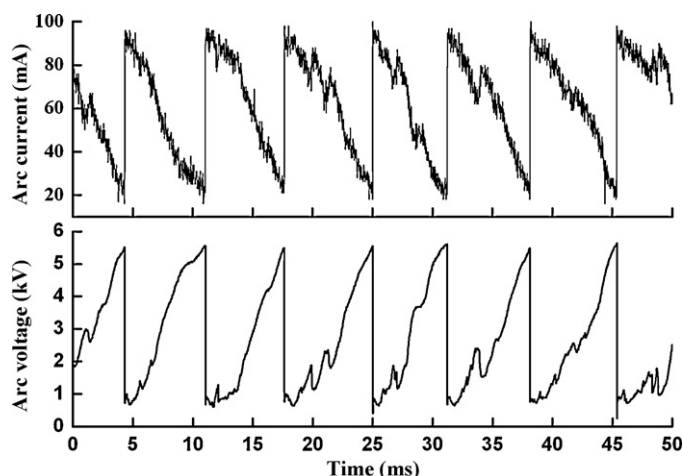


Fig. 3. Arc voltage and current signals of nitrogen gliding arc discharge.

applications: VOCs abatement [13–16], degradation of wastewater [17–20], hydrogen production [21–22].

3. Results and discussion

The destruction of four kinds of PAHs has been investigated varying carrier gas and external resistance. Results are expressed in terms of PAHs destruction rate (η_d) and energy efficiency (η_e), which are defined as follows:

$$\eta_d(\%) = \frac{X_{in} - X_{out}}{X_{in}} \times 100\% \quad (1)$$

$$\eta_e(\text{mg/J}) = \frac{(X_{in} - X_{out}) \times f_{\text{gas}}}{P_{GA}} \quad (2)$$

where X_{in} is the initial PAHs concentration, X_{out} is the final PAHs concentration, f_{gas} is the carrier gas flow rate and P_{GA} is the power of gliding arc plasma. In experiments, one parameter is kept constant while another parameter is varied.

The destruction rates of these four kinds of PAHs under all the experimental conditions are presented in Figs. 5 and 6. In Fig. 5, we can observe two different decomposition rate ranges: for AcP, the destruction rate varies from 61.4% to 93.5%; for Flu, the destruction rate varies from 59.4% to 93.1%. When the working gas is oxygen and the external resistance is 50 k Ω , the destruction rate can be achieved up to the highest independent on the type of PAHs. The

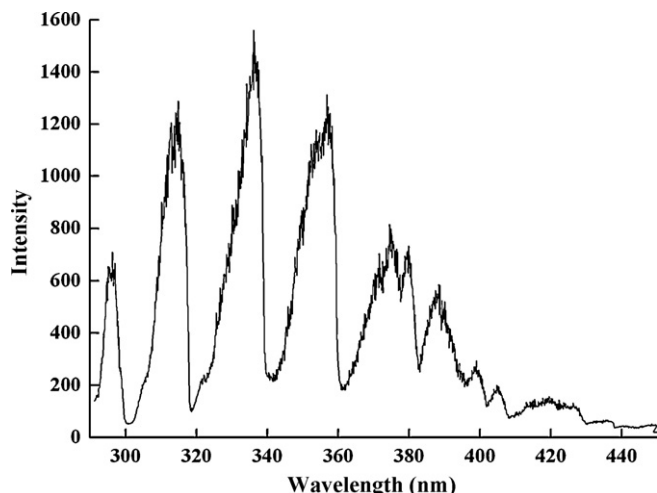


Fig. 4. Emission spectrum from nitrogen gliding arc discharge.

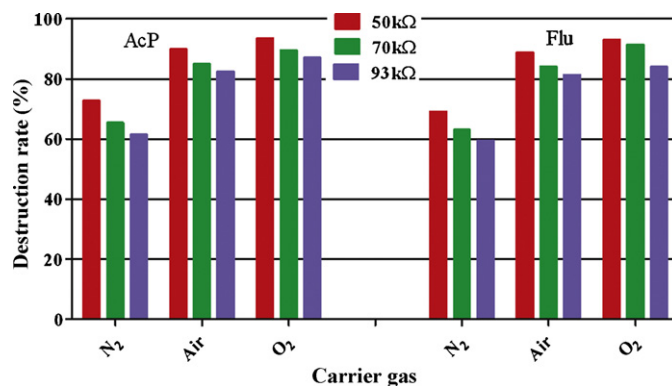


Fig. 5. Destruction rates of AcP and Flu under different experimental conditions: The initial concentrations of AcP and Flu are 0.63 mg/l and 0.25 mg/l, respectively.

influence of carrier gas and external resistance on the decomposition performance by the gliding arc plasma can be also found in Fig. 5. Increased destruction rates of AcP and Flu are observed as oxygen concentration in working gas increases or external resistance decreases. This phenomenon suggests that the treatment process in gliding arc can be enhanced by raising oxygen concentration or reducing external resistance.

As shown in Fig. 6, destruction rate ranges of AnT and Pyr are 79.1–97.4% and 77.4–97.6%, respectively. The highest destruction rates of AnT and Pyr are 97.4% and 97.6%, respectively, when oxygen is used as working gas and the external resistance is 50 k Ω . Compared with AcP and Flu destruction experiments, relative higher decomposition rates in these two sets of experiment are achieved. The effects of carrier gas and external resistance on AnT and Pyr destruction processes are also the same, which is in agreement with results of the experiments concerning with AcP and Flu destruction.

A few of literatures were concerning the destruction or removal of PAH from flue gas, and most of them focused on the absorption method by various carbonaceous materials. However the high removal efficiency achieved by the absorption means the initial concentration of PAHs in flue gas were very low [23]. Furthermore, this kind of method cannot destruct the pollutant, which would cause the secondary pollution. For some other methods emerged in recent years, Nair et al. have used the pulsed corona discharges to remove tar from biomass-derived fuel gas. Naphthalene removal efficiency can be achieved up to 90% when the energy density was over 400 J/l [24]. Ostapczuk et al. have utilized electron beam for destruction of gas phase naphthalene and acenaphthene and gained G-values of 1.66 and 3.72 mol/100 eV for naphthalene and acenaphthene at the dose of 1 kGy [25].

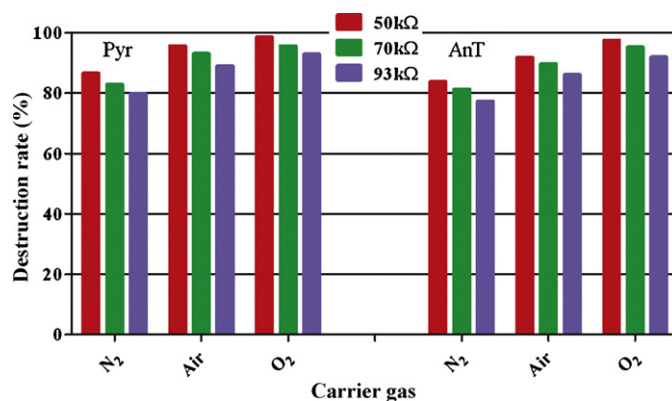


Fig. 6. Destruction rates of AnT and Pyr under different experimental conditions: the initial concentration of AnT and Pyr is 0.023 mg/l and 0.015 mg/l, respectively.

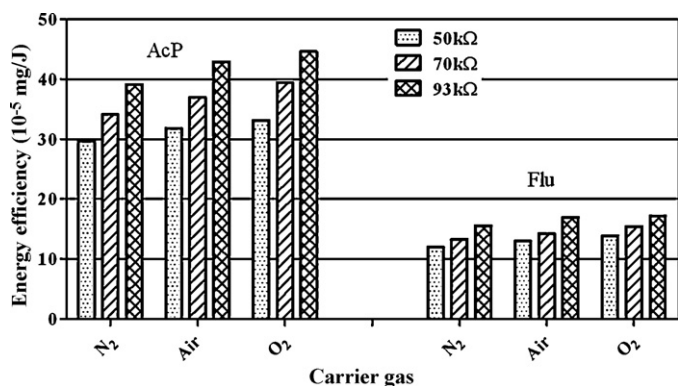


Fig. 7. Destruction energy efficiencies of AcP and Flu under different experimental conditions: The initial concentrations of AcP and Flu are 0.63 mg/l and 0.25 mg/l, respectively.

The significant influence of working gas on PAHs destruction process can be ascribed to participation of oxygen in pollutants decomposition reactions. Compared with nitrogen discharge, oxygen discharge has numerous reactive species such as O_2^+ , O^+ and O_3 . These species in oxygen plasma, which have stronger oxidizability than the radicals generated in nitrogen plasma, promote the PAHs degradation process. According to the circuit arrangement of gliding arc plasma generation, it is known that arc current and power decrease with the increasing of external resistance [26]. Reduction of gliding arc length, as well as the yield of energetic electrons and active species induced by decreasing of arc current and power inhibits destruction processes.

Due to the various V_p (vapor pressure) of four kinds of PAHs, the initial concentration of PAHs are not the same. Compared with destruction rates of AcP and Flu, the destruction rates of AnT and Pyr are much higher. This result can be ascribed to the much lower initial concentration of AnT and Pyr. The V_p of AnT and Pyr are much lower than that of AcP and Flu. The target molecule in lower concentration sharing more energetic electrons and reactive species leads to the higher decomposition rate. In the experiments of AcP and Flu destruction, however the lower initial concentration of Flu, the AcP destruction rates are slightly higher than those of Flu under all working conditions, which suggests AcP is more easily to be destroyed in plasma than Flu. Brubaker and Hites have also found that AcP is more active than Flu in their experiments about the reaction between OH radical and PAHs. They have found the reaction rate constant k of the reaction between OH and AcP ($5.8 \times 10^{-11} \text{ m}^3 \text{ molecule}^{-1} \text{ s}^{-1}$) is larger than that of the reaction concerning with Flu ($1.1 \times 10^{-11} \text{ m}^3 \text{ molecule}^{-1} \text{ s}^{-1}$) at the same condition [27].

Destruction energy efficiencies under different working conditions are presented in Figs. 7 and 8. As one can observe from Fig. 7, the energy efficiency of AcP destruction process varies from $3 \times 10^{-4} \text{ mg/J}$ to $4.5 \times 10^{-4} \text{ mg/J}$, while the range of Flu destruction energy efficiency is 1.2×10^{-4} – $1.7 \times 10^{-4} \text{ mg/J}$. Destruction energy efficiency increases with the increasing of external resistance. As the resistance value increases, the transition from equilibrium to non-equilibrium is promoted [26], which leads to the decrease of energy cost in destruction process. Destruction energy efficiency can be achieved up to the highest when oxygen is used as working gas and the external resistance is 93 kΩ. The AcP destruction energy efficiency is always larger than that of Flu under the same experimental conditions, which can be ascribed to the relative higher initial concentration of AcP. However the high destruction rates of AnT and Pyr, the destruction energy efficiency are very low which can be observed in Fig. 8. Compared with AcP

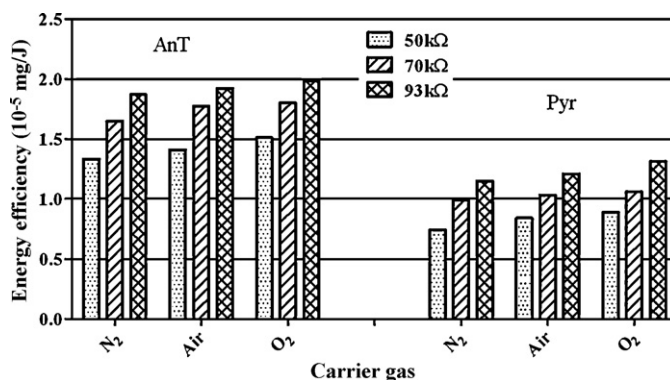


Fig. 8. Destruction energy efficiencies of AnT and Pyr under different experimental conditions: The initial concentration of AnT and Pyr is 0.023 mg/l and 0.015 mg/l, respectively.

and Flu destruction processes, the destruction energy efficiencies of AnT and Pyr are smaller than one tenth of those. The highest destruction energy efficiencies of AnT and Pyr are $2.0 \times 10^{-5} \text{ mg/J}$ and $1.3 \times 10^{-5} \text{ mg/J}$, respectively. It is possible to state that the much lower initial concentrations of AnT and Pyr result in the high energy cost and only small part of energy provided by gliding arc plasma is utilized for the treatment of AnT and Pyr. In order to prove this deduction, the experiments of simultaneous treatment with four kinds of PAHs are carried out at the same initial concentration level. Figs. 9 and 10 show the destruction rates of four targets and the energy efficiencies under different working conditions, respectively. It can be found that the influences of external resistance on destruction rate and energy efficiency in these simultaneous destruction experiments are the same as the above experiments. Although slight lower decomposition rates of AnT and Pyr can be observed in Fig. 9, the energy efficiency is as high as $6.24 \times 10^{-4} \text{ mg/J}$. This result suggests some part of energy in discharge are not utilized when using gliding arc plasma to treat with AnT and Pyr at low initial concentrations. In fact, the initial concentrations of AnT and Pyr in this study are much higher than the PAHs concentration in flue gas from waste incinerator [1]. Therefore, from an economic point of view, it is suggested that the destruction energy efficiency of gliding arc plasma would be improved by treating pollutants with higher concentration.

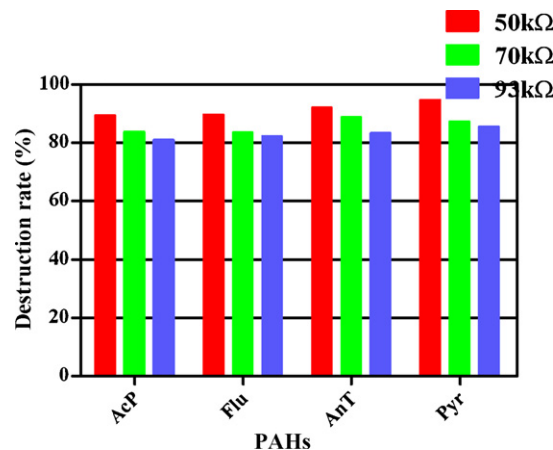


Fig. 9. Destruction rates of four kinds of PAHs in the air discharge: The initial concentrations of AcP, Flu, AnT and Pyr are 0.67 mg/l, 0.21 mg/l, 0.02 mg/l and 0.013 mg/l, respectively.

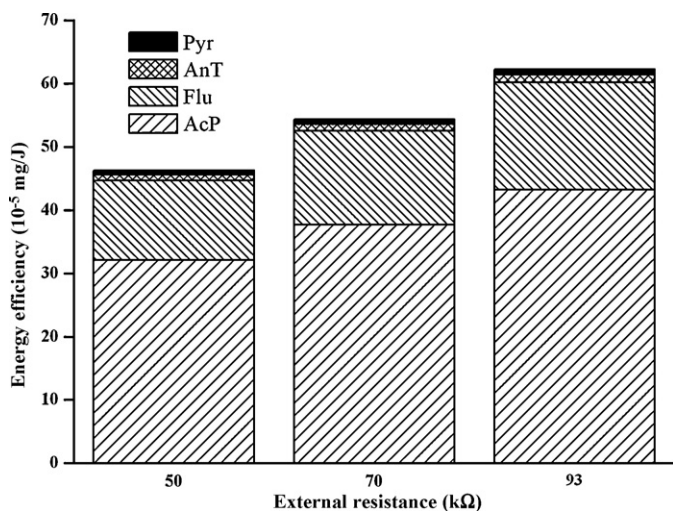


Fig. 10. Destruction energy efficiencies of four kinds of PAHs in the air discharge: The initial concentrations of AcP, Flu AnT and Pyr are 0.67 mg/l, 0.21 mg/l, 0.02 mg/l and 0.013 mg/l, respectively.

4. Destruction mechanism

All the identified post-destroyed products are listed in Table 1. Possible destruction mechanisms in different gas discharge are discussed based on the experimental results.

In nitrogen discharge processes, HCN is the main gas phase product. And HCN concentrations in AcP and Flu degradation processes are in range from 0.03 mg/l to 0.06 mg/l. For the much lower concentrations of AnT and Pyr, HCN is a trace product. In the nitrogen discharge, N_2^* and N_2^+ are also generated in plasma area via reactions (R1) and (R2), which has been observed by Delair et al. [28].

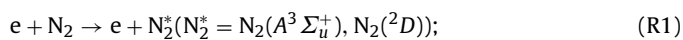
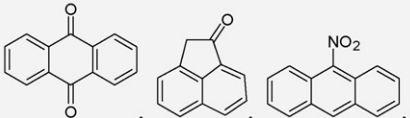
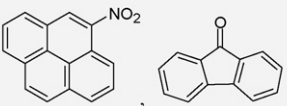
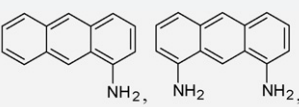
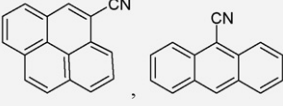
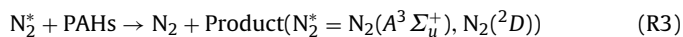


Table 1
Compounds identified in post-destroyed products.

Carrier gas	Products
Oxygen	CO ₂ , CO, H ₂ O, O ₃ 
Air	 CO ₂ , CO, H ₂ O, NO, NO ₂ 
Nitrogen	 HCN, soot

Excited state of N_2 and N_2^+ ion can directly react with PAHs which initiates the PAHs degradation via reactions (R3) and (R4) [29].



Additionally, high energy electrons abounds in the discharge area [28], and the mean energy of electrons in the gliding arc plasma region (1–3 eV) is high enough to dissociate the C–H bonds of targets. Therefore, it is possible to state that the reactions between PAHs and nitrogen-derived radicals and electron dissociation govern the PAHs destruction process in the nitrogen discharge, including charge transfer reaction, ring cleavage and C–H bond dissociation. Among the by-products, trace organic compounds with N-containing substituent ($-NH_2$, $-CN$) and HCN are identified, which suggests N react with intermediates in the destruction process and CN radical would recombine with intermediates. Blin-Simiand et al. have also found the possibility of reactions between CN radical and phenyl or between CN and methyl-phenyl in toluene destruction process by DBD discharge [30]. Some brown aerosol deposition on the inner surface of quartz reactor is also observed in all the nitrogen discharge experiments, which may indicates PAHs agglomeration reaction and soot formation take place in the decomposition process [31]. Although considerable destruction rates achieved in the nitrogen discharge, HCN generation and brown aerosol formation have negative impact on this treatment method.

In the oxygen discharge, the products are distinct from those in the nitrogen discharge. Since the combination of strong oxidation of oxygen-derived radicals and electron impact, the products are mainly CO₂, H₂O and CO and brown aerosol deposition is not observed during the experiments. Due to relative higher concentration of oxygen, some of oxygen molecules are first excited by electron impact via reactions (R5) and (R6).



Meanwhile, energetic electrons also attack the C–H bond of PAHs to generate unstable intermediates, which can be quickly oxidized by some radicals (O^* , O_2^* , OH etc) to the final products. In the AcP and Flu oxygen discharge destruction experiments, the concentrations of CO₂ and CO among the products are listed in Table 2. The carbon balance value B_c can be calculated by following equation:

$$B_c = \frac{[CO_2] + [CO]}{n_c \times [X_{in} - X_{out}]} \quad (3)$$

where n_c is the number of carbon atom in a PAHs molecule. For AcP and Flu, n_c is equal to 12 and 13, respectively. The values of B_c are above 90% independent of external resistance in oxygen discharge, which indicates that the main carbonaceous products of PAHs destruction process in oxygen discharges are CO and CO₂. In these four kinds of PAHs destruction experiments, no oxidized polycyclic aromats were detected in oxygen discharges, the reasons of which may be both low concentrations of these PAHs and the strong oxidizability of the oxygen discharge. In our previous study, [8] for a relative higher initial concentration of naphthalene (1.32 mg/l) and a larger flow rate (6.8 l/min), some trace indistinguishable aromatic and C–O containing hydrocarbon were detected in a destruction process by an oxygen discharge. In the other aspect, oxygen-derived radicals such as O, $O(^1D)$, $O(^3P)$ and O₃ are abounded in the oxygen discharge. CO and CO₂ concentrations among the products in the oxygen discharge listed in Table 3 indicated that more than 90% of carbon in PAHs is oxidized to CO and CO₂. Possibly, the oxidized polycyclic aromatics as intermediates are destroyed in the oxygen discharge for strong oxidizability of the oxygen discharge.

Table 2
Concentrations of NO and NO₂ in air discharges.

	AcP			Flu			AnT			Pyr		
Resistance (kΩ)	50	70	93	50	70	93	50	70	93	50	70	93
NO (mg/l)	4.18	2.39	1.88	4.18	2.40	1.88	4.21	2.43	1.91	4.22	2.39	1.90
NO ₂ (mg/l)	1.03	0.65	0.40	1.02	0.66	0.39	1.05	0.68	0.41	1.05	0.67	0.43

Table 3
Yields of CO and CO₂ in AcP and Flu destruction experiments.

	Carrier gas					
	Oxygen			Air		
External resistance (kΩ)	93	70	50	93	70	50
	CO ₂ /CO	CO ₂ /CO	CO ₂ /CO	CO ₂ /CO	CO ₂ /CO	CO ₂ /CO
AcP experiments (mg/l)	1.36/0.22	1.45/0.22	1.5/0.25	1.15/0.2	1.25/0.2	1.32/0.22
%C of the initial C (%)	62.6/16.0	66.9/16.0	69.2/18.1	53.0/14.5	57.6/14.5	60.1/16.0
Flu experiments (mg/l)	0.53/0.07	0.58/0.07	0.6/0.07	0.41/0.07	0.44/0.08	0.49/0.08
%C of the initial C (%)	61.0/12.7	66.8/12.7	69.1/12.7	47.2/12.7	50.8/15.7	56.4/14.5

As in the nitrogen and oxygen discharges, the PAHs removal process under air condition is also initiated by electron dissociation and reactions with the excited state of background gas molecule. Because of the reaction between nitrogen and oxygen in plasma, more reactions are involved in PAHs destruction process in the air discharge. Besides CO₂, CO and H₂O, NO and NO₂ as unfavorable gas phase products can be identified in air discharge products. In the air discharge, the reaction of oxygen and nitrogen leads to the formation of NO_x. The concentrations of NO_x in these experiments are listed in Table 2, which indicates that the concentration of NO is much larger than that of NO₂. The concentrations of NO and NO₂ in air discharges are listed in Table 3. NO concentrations (1.88–4.22 mg/l) are much higher than those of NO₂ (0.40–1.05 mg/l) in all experimental conditions. Furthermore, increased concentrations of NO and NO₂ are observed as external resistor value decreased, which can be ascribed to the larger discharge current and discharge energy resulted by a smaller external resistor value. Since very low concentrations of PAHs, the influence of PAHs species on oxides of nitrogen generation is limited.

The trace compounds with NO₂ substituent listed in Table 1 are also detected by GC/MS, which indicates the reactions take place between NO_x and intermediates. Hence, the simplified PAHs destruction pathway probably includes the reaction channels in oxygen discharge and nitrogen discharge and the reaction between NO_x and intermediates. Due to the lack of kinetic data for NO_x interaction with PAHs, it is complicated to evaluate the contribution of NO_x in PAHs destruction process. However, it is possible to state the reaction channels between O radical and PAHs play a vital role in removal process, which can result in a higher destruction rate than that in nitrogen discharge. For AcP and Flu destruction experiments, the concentrations of CO₂ and CO among the products generated in air discharge are listed in Table 2. It can be found that the values of B_c are about 85%, which are lower than those of oxygen discharge.

5. Conclusion

The experimental study of four kinds of PAHs i.e. AcP, Flu, AnT and Pyr destruction processes using dc gliding arc gas discharge with different carrier gases and external resistances has been carried out, which indicates PAHs can be efficiently removed by gliding arc plasma. Destruction process can be promoted by reducing external resistance or raising oxygen concentration in carrier gas. Destruction rates of these targets can be achieved up to 93.5%, 93.1%, 97.5% and 98.5%, respectively, with the carrier gas of oxygen and external resistance of 50 kΩ. Destruction energy efficiency increases with the increasing of external resistance, which can be achieved to the highest under oxygen condition. Due to the

low initial concentration, the energy efficiency is very low in the AnT and Pyr destruction processes. In the simultaneous removal of four kinds of PAHs experiments, the energy efficiency is achieved up to 6.24×10^{-4} mg/J. It is suggested that the destruction energy efficiency of gliding arc plasma would be improved by treating pollutants with higher concentration. Energetic electron impact and reaction with radicals generated in plasma region play a dominant role in decomposition processes under different background gases conditions.

Acknowledgement

We thank the support of National Nature Science Foundation of China (50976099).

References

- [1] K. Yasuda, M. Takahashi, The emission of polycyclic aromatic hydrocarbons from municipal solid waste incinerators during the combustion cycle, *J. Air Waste Manage. Assoc.* 48 (1998) 441–447.
- [2] L.H. Keith, W.A. Telliard, Priority pollutants I – a perspective view, *Environ. Sci. Technol.* 13 (1979) 416–423.
- [3] A.L. Juhász, R. Naidu, Bioremediation of high molecular weight polycyclic aromatic hydrocarbons: a review of the microbial degradation of benzo[a]pyrene, *Int. Biodeterior. Biodegrad.* 45 (2000) 57–88.
- [4] K. Nam, W. Rodriguez, J.J. Kukor, Enhanced degradation of polycyclic aromatic hydrocarbons by biodegradation combined with a modified Fenton reaction, *Chemosphere* 45 (2001) 11–20.
- [5] L.H. Zhang, P.J. Li, Z.Q. Gong, X.M. Li, Photocatalytic degradation of polycyclic aromatic hydrocarbons on soil surfaces using TiO₂ under UV light, *J. Hazard. Mater.* 158 (2008) 478–484.
- [6] B.Y. Chung, J.Y. Cho, C.H. Song, B.J. Park, Degradation of naturally contaminated polycyclic aromatic hydrocarbons in municipal sewage sludge by electron beam irradiation, *Bull. Environ. Contam. Toxicol.* 81 (2008) 7–11.
- [7] C.M. Du, J.H. Yan, X.D. Li, B.G. Cheron, X.F. You, Y. Chi, M.J. Ni, K.F. Cen, Simultaneous removal of polycyclic aromatic hydrocarbons and soot particles from flue gas by gliding arc discharge treatment, *Plasma Chem. Plasma Process.* 26 (2006) 517–525.
- [8] L. Yu, X.D. Li, X. Tu, Y. Wang, S.Y. Lu, J.H. Yan, Decomposition of naphthalene by dc gliding arc gas discharge, *J. Phys. Chem. A* 114 (2010) 360–368.
- [9] K. Urashima, J.S. Chang, Removal of volatile organic compounds from air streams and industrial flue gases by non-thermal plasma technology, *IEEE Trans. Dielectr. Electr. Insul.* 7 (2000) 602–614.
- [10] H.L. Chen, H.M. Lee, S.H. Chen, M.B. Chang, S.J. Yu, S.N. Li, Removal of volatile organic compounds by single-stage and two-stage plasma catalysis systems: a review of the performance enhancement mechanisms, current status, and suitable applications, *Environ. Sci. Technol.* 43 (2009) 2216–2227.
- [11] C.M. Du, J.H. Yan, B. Cheron, Decomposition of toluene in a gliding arc discharge plasma reactor, *Plasma Sources Sci. Technol.* 16 (2007) 791–797.
- [12] A. Fridman, S. Nester, L.A. Kennedy, A. Saveliev, O. Mutaf-Yardimci, Gliding arc gas discharge, *Prog. Energy Combust. Sci.* 25 (1999) 211–231.
- [13] K. Krawczyk, B. Ulejczyk, H.K. Song, A. Lamenta, B. Paluch, K. Schmidt-Szalowski, Plasma-catalytic reactor for decomposition of chlorinated hydrocarbons, *Plasma Chem. Plasma Process.* 29 (2009) 27–41.

- [14] Z. Bo, J.H. Yan, X.D. Li, Y. Chi, K.F. Cen, Scale-up analysis and development of gliding arc discharge facility for volatile organic compounds decomposition, *J. Hazard. Mater.* 155 (2008) 494–501.
- [15] A. Indarto, D.R. Yang, J.W. Choi, H. Lee, H.K. Song, Gliding arc plasma processing of CO₂ conversion, *J. Hazard. Mater.* 146 (2007) 309–315.
- [16] A. Czernichowski, Gliding arc – applications to engineering and environment control, *Pure Appl. Chem.* 66 (1994) 1301–1310.
- [17] L. Yu, J.H. Yan, X. Tu, X.D. Li, S.Y. Lu, K.F. Cen, Effect of water on gliding arc discharge fluctuation, *EPL (Europhys. Lett.)* 83 (2008) 45001.
- [18] J.L. Brisset, D. Moussa, A. Doubla, E. Hnatiuc, B. Hnatiuc, G.K. Youbi, J.M. Herry, M. Naitali, M.N. Bellon-Fontaine, Chemical reactivity of discharges and temporal post-discharges in plasma treatment of aqueous media: examples of gliding discharge treated solutions, *Ind. Eng. Chem. Res.* 47 (2008) 5761–5781.
- [19] B. Benstaali, D. Moussa, A. Addou, J.L. Brisset, Plasma treatment of aqueous solutes: some chemical properties of a gliding arc in humid air, *Eur. Phys. J. Appl. Phys.* 4 (1998) 171–179.
- [20] X. Tu, L. Yu, J.H. Yan, K.F. Cen, B.G. Cheron, Dynamic and spectroscopic characteristics of atmospheric gliding arc in gas-liquid two-phase flow, *Phys. Plasmas* 16 (2009) 113506–113515.
- [21] N. Rueangjitt, T. Sreethawong, S. Chavadej, Reforming of CO₂-containing natural gas using an AC gliding arc system: effects of operational parameters and oxygen addition in feed, *Plasma Chem. Plasma Process.* 28 (2008) 49–67.
- [22] S.C. Kim, Y.N. Chun, Experimental study on partial oxidation of methane to produce hydrogen using low-temperature plasma in AC Glidarc discharge, *Int. J. Energy Res.* 32 (2008) 1185–1193.
- [23] A.M. Mastral, T. Garcia, R. Murillo, M.S. Callen, J.M. Lopez, M.V. Navarro, PAH mixture removal from hot gas by porous carbons. From model compounds to real conditions, *Ind. Eng. Chem. Res.* 42 (2003) 5280–5286.
- [24] S.A. Nair, A.J.M. Pemen, K. Yan, E.J.M. van Heesch, K.J. Ptasinski, A.A.H. Drinkenburg, Chemical processes in tar removal from biomass derived fuel gas by pulsed corona discharges, *Plasma Chem. Plasma Process.* 23 (2003) 665–680.
- [25] A. Ostapczuk, T. Hakoda, A. Shimada, T. Kojima, Naphthalene and acenaphthene decomposition by electron beam generated plasma application, *Plasma Chem. Plasma Process.* 28 (2008) 483–494.
- [26] O. Mutaf-Yardimci, A.V. Saveliev, A.A. Fridman, L.A. Kennedy, Thermal and non-thermal regimes of gliding arc discharge in air flow, *J. Appl. Phys.* 87 (2000) 1632–1641.
- [27] W.W. Brubaker, R.A. Hites, OH reaction kinetics of polycyclic aromatic hydrocarbons and polychlorinated dibenzo-p-dioxins and dibenzofurans, *J. Phys. Chem. A* 102 (1998) 915–921.
- [28] L. Delair, J.L. Brisset, B.G. Cheron, Spectral electrical and dynamical analysis of a 50 Hz air gliding arc, *High Temp. Mater. Process* 5 (2001) 381–402.
- [29] V.A. Bityurin, E.A. Filimonova, G.V. Naidis, Simulation of naphthalene conversion in biogas initiated by pulsed corona discharges, *IEEE Trans. Plasma Sci.* 37 (2009) 911–919.
- [30] N. Blin-Simiand, F. Jorand, L. Magne, S. Pasquiers, C. Postel, J.R. Vacher, Plasma reactivity and plasma-surface interactions during treatment of toluene by a dielectric barrier discharge, *Plasma Chem. Plasma Process.* 28 (2008) 429–466.
- [31] M. Frenklach, Reaction mechanism of soot formation in flames, *Phys. Chem. Chem. Phys.* 4 (2002) 2028–2037.